Journal of Solid Mechanics Vol. 4, No. 3 (2012) pp. 237-251

Displacements and Stresses in Pressurized Thick FGM Cylinders with Varying Properties of Power Function Based on HSDT

M. Ghannad, H. Gharooni*

Department of Mechanical Engineering, Shahrood University of Technology, Shahrood, Iran

Received 25 June 2012; accepted 29 August 2012

ABSTRACT

Using the infinitesimal theory of elasticity and analytical formulation, displacements and stresses based on the high-order shear deformation theory (HSDT) is presented for axisymmetric thick-walled cylinders made of functionally graded materials under internal and/or external uniform pressure. The material is assumed to be isotropic heterogeneous with constant Poisson's ratio and radially varying elastic modulus continuously along the thickness with a power function. At first, general governing equations of the FGM thick cylinders are derived by assumptions of the high-order shear deformation theory. Following that, the set of non-homogenous linear differential equations with constant coefficients, for the cylinder under the generalized clamped-clamped conditions have been solved analytically and the effect of loading and inhomogeneity on the stresses and displacements have been investigated. The results are compared with the findings of both first-order shear deformation theory (FSDT) and finite element method (FEM). Finally, the effects of higher order approximations on the stresses and displacements have been studied.

Keywords: Thick cylinders; Shear deformation theory; FGM; HSDT; FEM

1 INTRODUCTION

AXISYMMETRIC hollow cylinders are important in industries. In order to optimize the weight, mechanical strength, displacement and stress distribution of a shell, one approach is to use shells with functionally graded materials (FGMs). FGMs or heterogeneous materials are advanced composite materials with microscopically inhomogeneous characters. The first order shear deformation theory (FSDT) for homogeneous thick cylindrical shells was expressed by Mirsky-Hermann [1]. Reddy and Liu developed a simple higher order shear deformation shell theory, in which the transverse shear strains are assumed to be parabolically distributed across the shell thickness and which contains the same number of dependent unknowns as in the first-order shear deformation theory, and no shear correction factors are required [2]. Greenspon compared the results of different theories of thick-walled cylindrical shells [3]. Fukui and Yamanaka used the Navier solution for derivation of the governing equation of a thick-walled FGM tube under internal pressure and solved the obtained equation numerically by means of the Runge-Kutta method [4]. Simkins used the FSDT for determining displacement in a long and thick tube subjected to moving loads [5]. Eipakchi et. al. have investigated the governing equations of homogeneous cylinders with variable thickness using FSDT and represent the solution of the equations using perturbation theory [6]. They further extended their previous work by considering homogenous and isotropic conical shells with variable thickness using FSDT and SSDT (second-order shear deformation theory) and solved the conducted equations by perturbation theory [7].

* Corresponding author. Tel.: +98 915 305 6995.
E-mail address: Gharooni.hamed@gmail.com (H.Gharooni).

Hongjun et al. indicated the exact solution of FGM hollow cylinders in the state of plane strain with exponential function of elasticity modulus along the radius [8]. Zhifei et al. analyzed heterogeneous cylindrical shells with power function of elasticity modulus by the usage of multilayer method with homogeneous layers [9]. Thick-walled FGM cylinders in plane strain state with exponentially-varying material properties were solved by Tutuncu using Frobenius method [10]. Ghannad et al. provided a general axisymmetric solution of thick FGM cylinders based on plane elasticity theory (PET) in the state of plane stress, plane strain and closed cylinder [11]. They investigated the general solution of the thick FGM cylinders with power function elastic modulus based on FSDT and compare the results with PET solution [12]. Zamani Nejad et al. developed 3-D set of field equations of FGM thick shells of revolution in curvilinear coordinate system by tensor calculus [13]. Ghannad et al. derived the governing differential equations of axisymmetric thick truncated conical shells based on first-order shear deformation theory (FSDT) and the virtual work principle [14]. They used the matched asymptotic method (MAM) of the perturbation theory for converting resulted equations into a system of algebraic equations and two systems of differential equations with constant coefficients. They presented the general method of derivation and the analysis of internally pressurized thick-walled cylinders with clamped-clamped ends [15]. Eipakchi calculated stresses and displacements of a thick conical shell with varying thickness under nonuniform internal pressure analytically using third-order shear deformation theory [16]. Ghannad et al. presented a closed form analytical solution for clamped-clamped thick cylindrical shells with variable thickness subjected to constant internal pressure based on the first-order shear deformation theory (FSDT) [17].

It is observed that the analysis of pressurized thick FGM cylinders based on higher order shear deformation theory have not been studied in the previous literatures. Furthermore, the results of the previous analysis of the cylindrical shells show that FSDT is not an appropriate theory for stress analysis, means that the accuracy of the stresses (especially radial stresses),unlike displacements which have been calculated directly by SDT, are not acceptable. In order to improve the approximation of shear deformation theory and taking into account the effect of shear stresses and strains, the general method of derivation and the analysis of an internally and/or externally pressurized thick-walled cylindrical shells made up of functionally graded material with constant Poisson's ratio and radially varying elastic modulus with a power function have been presented using HSDT. The coefficients matrices of the governing equations have been derived in the unique abbreviated form. The obtained equations are solved under the generalized clamped-clamped conditions. Furthermore, the effect of loading and inhomogeneity on the stresses and displacements has been investigated. The results are compared with the findings of both SDT and FEM. Finally, the efficiency and accuracy of the higher-order shear deformation theory into the lower one have been shown.

2 PROBLEM FORMULATION

The basic elements in shear deformation theory (SDT), the straight lines perpendicular to the central axis of the cylinder do not necessarily remain unchanged after loading and deformation, suggest that the deformations are axisymmetric and change along the longitudinal direction of cylinder. In other words, the elements have rotation, and the shear strain is not zero. The displacement field is assumed as a polynomial of a variable (z) through the thickness. As the number of terms in the polynomial function increase, the approximate solution will be improved. The high-order shear deformation theory (HSDT) is employed to simulate the deformation of every layer of the cylinder [16].

The parameter r is the radius of every layer of cylinder which can be replaced in terms of radius of mid-plane R and distance of every layer with respect to mid-plane z as follows(see Fig. 1):

$$r = R + z \tag{1}$$

x and z are the length and the thickness variables. The parameters x and z have been changed in the following intervals:

$$0 \le x \le L \ , \ -\frac{h}{2} \le z \le +\frac{h}{2} \tag{2}$$

where h and L are the thickness and the length of the cylinder.

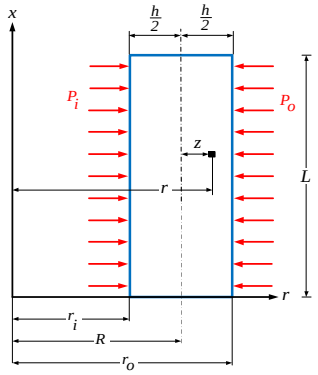

Fig. 1
Geometry of the thick pressurized cylindrical shell.

Based on HSDT, every component of deformation can be stated by variables that includes the displacement and rotation. For an axisymmetric cylindrical shell, axial and radial components of displacement field are assumed to be in the following form [16]:

$$\begin{cases} U_x = u_0(x) + zu_1(x) + z^2u_2(x) + z^3u_3(x) \\ U_\theta = 0 \\ U_z = w_0(x) + zw_1(x) + z^2w_2(x) + z^3w_3(x) \end{cases} \tag{3}$$

where $u_0(x)$ and $w_0(x)$ are the displacement components of the middle surface. Also, $u_1(x)$ and $w_1(x)$ are the rotations of the normal to the middle surface with respect to the x - and z - axes, respectively. u_0, u_1, u_2, u_3 and w_0, w_1, w_2, w_3 are the unknown functions of x used to determine the displacement field.

The mechanical kinematic relations in the cylindrical coordinates system for an axisymmetric cylinder are [16]:

$$\begin{cases} \varepsilon_x = \dfrac{\partial U_x}{\partial x} = \dfrac{du_0}{dx} + \dfrac{du_1}{dx}z + \dfrac{du_2}{dx}z^2 + \dfrac{du_3}{dx}z^3 \\ \varepsilon_\theta = \dfrac{U_z}{r} = \dfrac{w_0 + w_1z + w_2z^2 + w_3z^3}{R+z} \\ \varepsilon_z = \dfrac{\partial U_z}{\partial z} = w_1 + 2w_2z + 3w_3z^2 \\ \gamma_{xz} = \dfrac{\partial U_x}{\partial z} + \dfrac{\partial U_z}{\partial x} = \left(u_1 + \dfrac{dw_0}{dx}\right) + \left(2u_2 + \dfrac{dw_1}{dx}\right)z + \left(3u_3 + \dfrac{dw_2}{dx}\right)z^2 + \dfrac{dw_3}{dx}z^3 \end{cases} \tag{4}$$

Modulus of elasticity E is supposed to be a power function of the radial coordinate r which have been normalized as $\bar{r} = r/r_i$ and is assumed to vary as follows:

$$E(r) = E_i(\bar{r})^n = E_i\left(\frac{r}{r_i}\right)^n \tag{5}$$

Here, E_i is the modulus of elasticity at the inner surface r_i and n is the in homogeneity constant determined empirically. Generally, the Poisson's ratio, ν, for a thick-walled cylindrical pressure vessel of isotropic FGM varies in a small range. Furthermore, its effects on mechanical stresses are insignificant. For simplicity, the Poisson's ratio is assumed to be constant.

The range $-2 \le n \le +2$ to be used in the present study covers all the values of coordinate exponent encountered in the references cited earlier. However, these values for n do not necessarily represent a certain material.

Fig. 2 shows the distribution of normalized elasticity modulus with respect to the normalized radius in a heterogeneous cylinder for integer values of n.

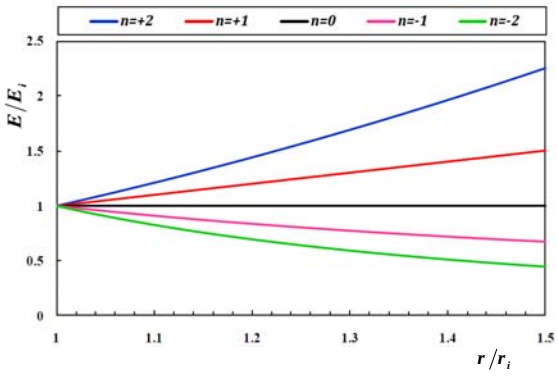

Fig. 2
Distribution of normalized elasticity modulus in FGM cylinder.

On the basis of the constitutive equations for inhomogeneous and isotropic materials, the stress-strain relations are as follows [2]:

$$\begin{cases} \begin{Bmatrix} \sigma_x \\ \sigma_\theta \\ \sigma_z \end{Bmatrix} = \begin{bmatrix} \lambda+2\mu & \lambda & \lambda \\ \lambda & \lambda+2\mu & \lambda \\ \lambda & \lambda & \lambda+2\mu \end{bmatrix} \begin{Bmatrix} \varepsilon_x \\ \varepsilon_\theta \\ \varepsilon_z \end{Bmatrix} \\ \tau_{xz} = \mu\gamma_{xz} \end{cases} \tag{6}$$

where λ and μ are the Lame's constants. Considering variable elasticity modulus for the FGM materials, these two parameters are as follows [2]:

$$\lambda = \frac{\nu E(z)}{(1+\upsilon)(1-2\upsilon)} \tag{7}$$

$$\mu = \frac{E(z)}{2(1+\upsilon)} \tag{8}$$

With substitution of r from Eq. (1) into Eq. (5), distribution of elasticity modulus may be re-written as a function of z:

$$E(z) = E_i\left(\frac{R+z}{r_i}\right)^n \tag{9}$$

The stress resultants are as follows [2]:

$$\begin{Bmatrix} N_x \\ N_\theta \\ N_z \end{Bmatrix} = \int_{-h/2}^{h/2} \begin{Bmatrix} \sigma_x\left(1+\frac{z}{R}\right) \\ \sigma_\theta \\ \sigma_z\left(1+\frac{z}{R}\right) \end{Bmatrix} dz \tag{10}$$

$$\begin{Bmatrix} M_x \\ M_\theta \\ M_z \end{Bmatrix} = \int_{-h/2}^{h/2} \begin{Bmatrix} \sigma_x\left(1+\frac{z}{R}\right) \\ \sigma_\theta \\ \sigma_z\left(1+\frac{z}{R}\right) \end{Bmatrix} z dz \tag{11}$$

$$\begin{Bmatrix} P_x \\ P_\theta \\ P_z \end{Bmatrix} = \int_{-h/2}^{h/2} \begin{Bmatrix} \sigma_x \left(1+\frac{z}{R}\right) \\ \sigma_\theta \\ \sigma_z \left(1+\frac{z}{R}\right) \end{Bmatrix} z^2 dz \tag{12}$$

$$\begin{Bmatrix} S_x \\ S_\theta \end{Bmatrix} = \int_{-h/2}^{h/2} \begin{Bmatrix} \sigma_x \left(1+\frac{z}{R}\right) \\ \sigma_\theta \end{Bmatrix} z^3 dz \tag{13}$$

$$Q_x = \int_{-h/2}^{h/2} \tau_{xz} \left(1+\frac{z}{R}\right) dz \tag{14}$$

$$M_{xz} = \int_{-h/2}^{h/2} \tau_{xz} \left(1+\frac{z}{R}\right) z dz \tag{15}$$

$$P_{xz} = \int_{-h/2}^{h/2} \tau_{xz} \left(1+\frac{z}{R}\right) z^2 dz \tag{16}$$

$$S_{xz} = \int_{-h/2}^{h/2} \tau_{xz} \left(1+\frac{z}{R}\right) z^3 dz \tag{17}$$

In order to drive the differential equations of equilibrium, the principle of virtual work have been used as:

$$\delta U = \delta W \tag{18}$$

where U is the total strain energy of the elastic body and W is the total external work due to internal and/or external pressure. The strain energy is

$$\begin{cases} U = \iiint_V U^* dV \ , \ dV = r dr d\theta dx = (R+z) dx d\theta dz \\ U^* = \frac{1}{2} \{\varepsilon\}^T \{\sigma\} = \frac{1}{2} (\sigma_x \varepsilon_x + \sigma_\theta \varepsilon_\theta + \sigma_z \varepsilon_z + \tau_{xz} \gamma_{xz}) \end{cases} \tag{19}$$

and the external work is

$$\begin{cases} W = \iint_S \left(\overrightarrow{f_{sf}} \cdot \vec{u} \right) dS \ , \ dS = r d\theta dx \\ \left(\overrightarrow{f_{sf}} \cdot \vec{u} \right) dS = \left(P_i r_i - P_o r_o \right) U_z d\theta dx \end{cases} \tag{20}$$

P_i and P_o are the horizontal pressures in the internal and external surfaces. Variation of the strain energy can be expressed as follows:

$$\begin{cases} \delta U = R \int_0^{2\pi} \int_0^L \int_{-h/2}^{h/2} \delta U^* \left(1+\frac{z}{R}\right) dz dx d\theta \\ \Rightarrow \frac{\delta U}{2\pi} = R \int_0^L \int_{-h/2}^{h/2} (\sigma_x \delta\varepsilon_x + \sigma_\theta \delta\varepsilon_\theta + \sigma_z \delta\varepsilon_z + \tau_{xz} \delta\gamma_{xz}) \left(1+\frac{z}{R}\right) dz dx \end{cases} \tag{21}$$

and the variation of the external work is

$$\begin{cases} \delta W = \int_0^{2\pi}\int_0^{L}\left[P_i r_i - P_o r_o\right]\delta U_z\, dx d\theta \\ \Rightarrow \dfrac{\delta W}{2\pi} = \int_0^{L}\left[P_i\left(R-\dfrac{h}{2}\right) - P_o\left(R+\dfrac{h}{2}\right)\right]\delta U_z\, dx \end{cases} \tag{22}$$

By substituting Eqs. (4), (6) and (9) into Eqs. (21) and (22) and by using Eq. (18), and carrying out the integration by parts, the equilibrium equations are obtained in the form of

$$\begin{cases} R\dfrac{dN_x}{dx} = F_{x_0}^P \\ R\dfrac{dM_x}{dx} - RQ_x = F_{x_1}^P \\ R\dfrac{dP_x}{dx} - 2RM_{xz} = F_{x_2}^P \\ R\dfrac{dS_x}{dx} - 3RP_{xz} = F_{x_3}^P \\ R\dfrac{dQ_x}{dx} - N_\theta = F_{z_0}^P \\ R\dfrac{dM_{xz}}{dx} - M_\theta - RN_z = F_{z_1}^P \\ R\dfrac{dP_{xz}}{dx} - P_\theta - 2RM_z = F_{z_2}^P \\ R\dfrac{dS_{xz}}{dx} - S_\theta - 3RP_z = F_{z_3}^P \end{cases} \tag{23}$$

where F^P stand for non-homogeneity of the governing equations which have been resulted from the loading of pressure. The subscript x and z in the right terms of each equation show the component of F^P along the axial and radial direction, respectively. we have:

$$\begin{cases} F_{x_i}^P = 0 \\ F_{z_i}^P = -Rf_{sf}\, z^i\left(1+\dfrac{z}{R}\right)\Big|_{z=\pm\frac{h}{2}} \end{cases} \qquad i = 0,1,2,3 \tag{24}$$

and the boundary conditions at the two ends of cylinder are

$$R\left[N_x\delta u_0 + M_x\delta u_1 + P_x\delta u_2 + S_x\delta u_3 + Q_x\delta w_0 + M_{xz}\delta w_1 + P_{xz}\delta w_2 + S_{xz}\delta w_3\right]_0^L = 0 \tag{25}$$

Eqs. (23) express the main governing equations based on the HSDT for the cylindrical shells under internal or external pressure. Eq. (25) is the boundary conditions which should be satisfied at two end of the cylinder.

In fact, Eqs. (23) are the set of differential equations. In order to solve the set of Eqs. (23), forces and moments should be written by the usage of Eqs. (10) to (17) in the terms of displacement field. Finally, a set of linear non-homogenous differential equations with constant coefficients would be resulted as follows:

$$[A]\frac{d^2}{dx^2}\{y\} + [B]\frac{d}{dx}\{y\} + [C]\{y\} = \{F\} \tag{26}$$

where $\{y\}$ is the unknown vector including the components of displacement field, $[A]_{8\times8}$, $[B]_{8\times8}$ and $[C]_{8\times8}$ are the coefficients matrices and $\{F\}$ is the force vector which can be expressed as the non-homogeneity of the set of differential equations.

Matrix $[C]$ is irreversible and its reverse is needed in the next calculations. In order to make $[C]^{-1}$, the first equation in the set of Eqs. (23) have been integrated.

$$RN_x = C_0 \tag{27}$$

In Eqs. (23), it is apparent that u_0 does not exist, but du_0/dx does. In Eq. (4), du_0/dx is needed to calculate displacements, therefore by assuming $du_0/dx = v$ as a new parameter which could be indicated in the following terms

$$u_0 = \int v dx + C_{15} \tag{28}$$

By the mentioned changes, the unknown vector $\{y\}$ in the set of differential Eqs. (23) can be rewritten as follows:

$$\{y\} = \{v \;\; u_1 \;\; u_2 \;\; u_3 \;\; w_0 \;\; w_1 \;\; w_2 \;\; w_3\}^T \tag{29}$$

Also non-homogeneity of the differential Eqs. (23) can be derived as follows:

$$\{F^p\} = \{F_{x_0} + C_0 \;\; F_{x_1} \;\; F_{x_2} \;\; F_{x_3} \;\; F_{z_0} \;\; F_{z_1} \;\; F_{z_2} \;\; F_{z_3}\}^T \tag{30}$$

The corresponding coefficient matrices $[A]$, $[B]$ and $[C]$ of new differential Eqs. (23) have been defined in Appendix.

3 ANALYTICAL SOLUTION

The Eq. (26) has the general solution $\{y\}_g$ and the particular solution $\{y\}_p$, as follows:

$$\{y\} = \{y\}_g + \{y\}_p \tag{31}$$

For the general solution, $\{y\}_g = \{V\}e^{mx}$ is substituted in homogeneous Eq. (26).

$$e^{mx}\left[m^2[A] + m[B] + [C]\right]\{V\} = \{0\} \tag{32}$$

Considering that e^{mx} is not equal to zero, the following determinant which is equal to zero would be resulted.

$$\left|m^2[A] + m[B] + [C]\right| = 0 \tag{33}$$

The above determinant is a sixteen-order polynomial which is a function of m, the roots of which are the eigenvalues m_i consist of 8 pairs of conjugated root where a pair of the roots is zero. Substituting the calculated eigenvalues in Eq. (32), the corresponding eigenvectors $\{V\}_i$ are obtained. Therefore, the general solution has been resulted.

$$\{y\}_g = \sum_{i=1}^{14} C_i \{V\}_i e^{m_i x} \tag{34}$$

Given that $\{F\}$ is comprised of constant parameters, for the non-homogenous part of solution of Eq. (26), the particular solution can be expressed as follows:

$$[C]\{y\}_p = \{F\} \Rightarrow \{y\}_p = [C]^{-1}\{F\} \tag{35}$$

Finally, the total solution is a summation of the general and the particular solution.

$$\{y\} = \sum_{i=1}^{14} C_i \{V\}_i e^{m_i x} + [C]^{-1}\{F\} \tag{36}$$

Constants $C_1,\ldots,C_{14}$ in the general solution and two constants C_0, C_{15} which have been resulted by the mathematical calculus will be obtained by applying eight boundary conditions.

Given that the two ends of the cylinder are clamped-clamped, then

$$\begin{cases} x=0 & \Rightarrow u_0 = u_1 = u_2 = u_3 = w_0 = w_1 = w_2 = w_3 = 0 \\ x=L & \Rightarrow u_0 = u_1 = u_2 = u_3 = w_0 = w_1 = w_2 = w_3 = 0 \end{cases} \tag{37}$$

4 RESULTS AND DISCUSSION

As a case study, we consider a thick cylinder whose elasticity modulus varies in radial direction and has the following characteristics: $r_i = 40\ mm$, $h = 20\ mm$ and $L = 0.8m$. The elasticity modulus at the internal radius and Poisson's ratio have values of $E_i = 200GPa$ and $\nu = 0.3$, respectively. The applied internal and external pressures are $P_i = P_o = 80MPa$. The analytical solution is carried out by writing the program in MAPLE 13.

In order to show the abilities of the presented analytical solution for analyzing a FG cylinder, a numerical solution has been investigated. The ANSYS 13 package was used in the static analysis of thick hollow cylinder with constant thickness. The PLANE 82 element in axisymmetric mode, which is an element with eight nodes and two translational degrees of freedom in the axial and radial directions per each node, was used for modeling. In order to consider the radial continuous varying of elastic modulus along the thickness of cylindrical shell with a power function, the thickness of cylinder has been divided to some homogeneous layers. Each layer's properties have been defined as a power function of the distance of layer's middle from internal layer. Finally the cylindrical shell consists of some coherent homogeneous layers whose properties at the contact location of the layers are the average of left and right limit of two layers' boundaries. Internal and external pressures are applied to the nodes of inner and outer layers, respectively. Clamped boundary conditions have been exerted by preventing the nodes around two ends of the cylinder from movement. In the next sections, the numerical and analytical results have been investigated for clamped-clamped boundary conditions.

4.1 Inhomogeneity and pressure effect

The distribution of the normalized radial displacement resulted from the numerical and analytical solution at middle of a cylinder under internal and external pressure is depicted in Figs.3 and 4, respectively. It is seen that for negative values of *n*, the displacements of FGM cylinders are higher than of a homogeneous cylinder. For positive values of *n*, the situation is reverse, i.e. the displacement is lower. The variation in the displacement of heterogeneous material is similar to that of homogenous material. It is obviously observed in Fig. 3 that the radial displacements have its maximum values in internal surface ($z = -h/2$). Although the radial displacement of the cylinder under external pressure has negative value unlike the cylinder under internal pressure, it is clearly seen that external pressure causes higher displacement than internal one.

Figs.5 and 6 show the distribution of the normalized radial and axial displacement along the axial in the middle surface of the cylinder under internal pressure for different inhomogeneity constants. The radial displacement at points away from the boundaries depends on radius and length. It's observed that middle of the cylinder has no axial

displacement. For $n<0$ axial displacements of the cylinder are more than homogeneous material while for $n>0$ is smaller.

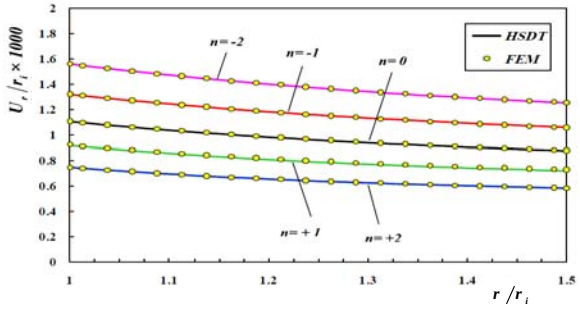

Fig. 3
Radial displacement distribution at middle of the cylinder under internal pressure.

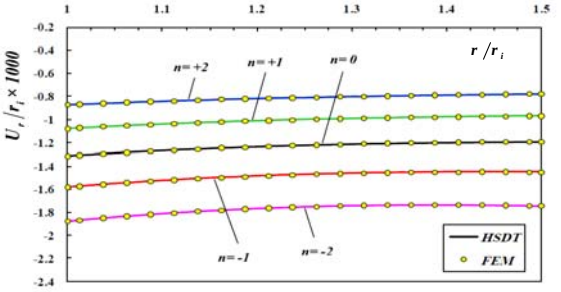

Fig. 4
Radial displacement distribution at middle of the cylinder under external pressure.

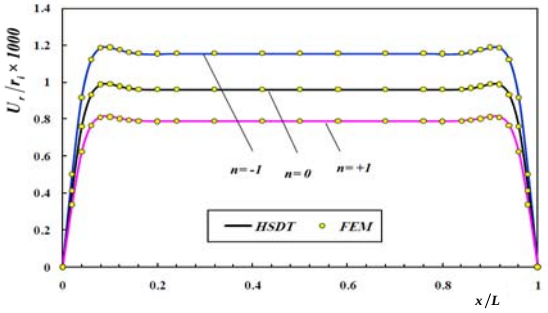

Fig. 5
Radial displacement distribution in the middle surface.

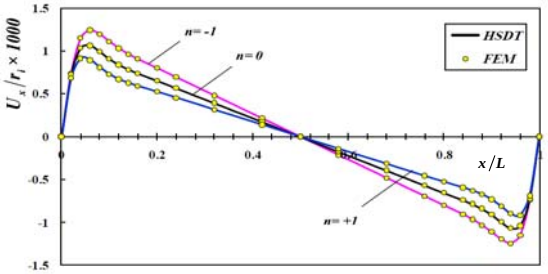

Fig. 6
Axial displacement distribution in middle surface.

Distribution of the normalized circumferential stress resulted from the numerical and analytical solution at the middle of the cylinder for internal and external pressure is shown in Figs.7 and 8. In the cylinder under internal pressure, the circumferential stress for negative values of n is higher than the homogenous materials at layers close to the internal surface while at the outer one, is less than the homogenous materials. For positive values of n the reverse holds true means that the heterogonous materials have less value of circumferential stress than the homogenous ones at inner surfaces and the higher value of stress at outer surfaces. Considering the negative

circumferential stress caused by the external pressure, the cylinder under external pressure shows the same behavior from the viewpoint of the absolute value of stress as the internal pressure for different value of n. The greatest circumferential stress of the cylinder under internal pressure occurs in the internal surface $(z=-h/2)$ for $n \geq 1.15$ and vice versa for the material with inhomogeneity constants of lower values while this limit decreases to the value of 0.9 for the cylinder under external pressure.

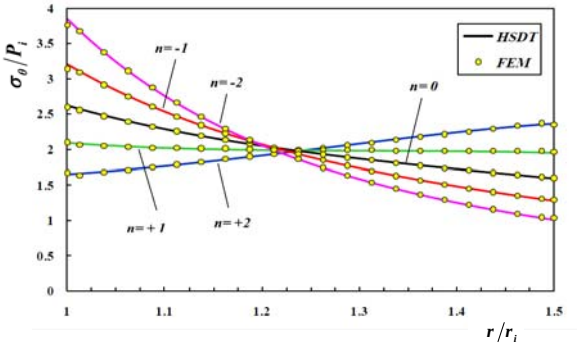

Fig. 7
Circumferential stress distribution at middle of the cylinder under internal pressure.

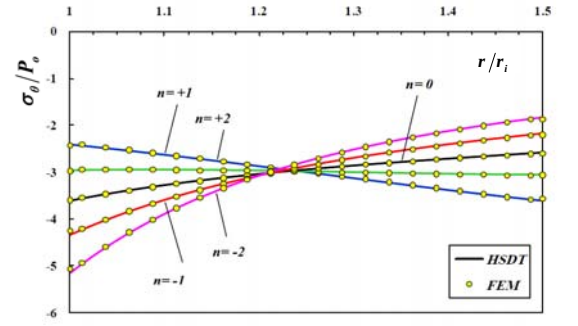

Fig. 8
Circumferential stress distribution at middle of the cylinder under external pressure.

Distribution of von Mises stress resulted from analytical solution in different layers for the cylinder under internal pressure is shown in Figs. 9 and 10 for $n=\pm 1$. The von Mises stress at all points depends on radius and length. The greatest von Mises stress of the cylinder under internal pressure occurs in the internal surface and from the internal layer to the external one these values decrease. For positive value of n unlike the negative one, the range of stresses shows small variation in different layers. It is obviously apparent that stress at points near the boundaries is different from the other areas under the effect of shear stresses resulted from boundary conditions. The results suggest that in points further away from the boundary it is possible to make use of the plane elasticity theory (PET).

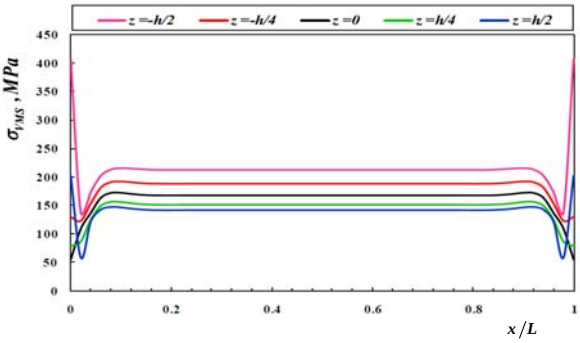

Fig. 9
von Mises stress distribution in different layers for $n=+1$.

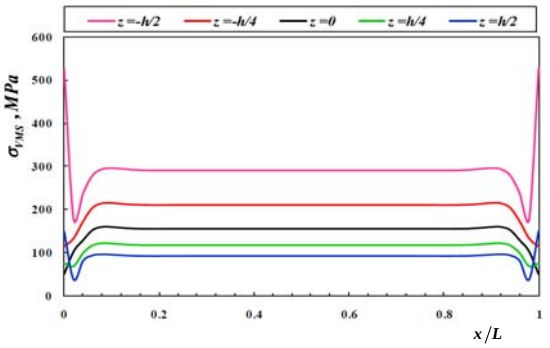

Fig. 10
von Mises stress distribution in different layers for $n=-1$.

Distribution of axial stress resulted from analytical solution in different layers of the cylinder under internal pressure is shown in Figs.11 and 12 for $n=\pm 1$. At points away from the boundaries, axial stress does not show significant differences in different layers, while at points near the boundaries, the reverse holds true.

Figs. 13 and 14 show the distribution of shear stress resulted from analytical solution along the longitude of cylinder under internal pressure for $n=\pm 1$ in different layers. It is obviously observed that there are shear stresses near two ends of the cylinder. The shear stress at points away from the boundaries at different layers is the same and trivial. However, at points near the boundaries, the stress is significant.

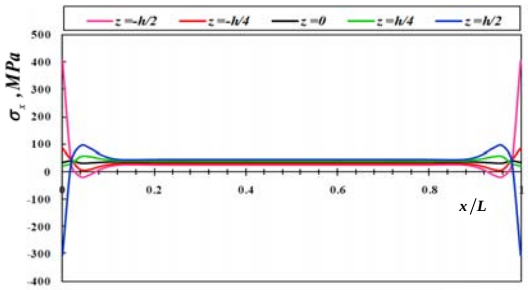

Fig. 11
Axial stress distribution in different layers for $n=+1$.

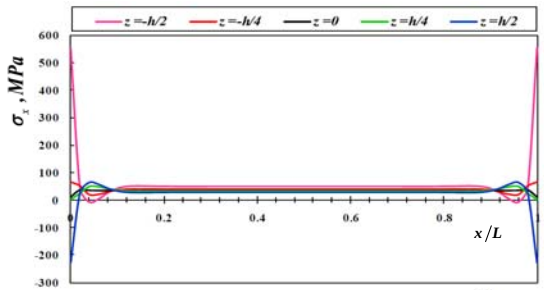

Fig. 12
Axial stress distribution in different layers for $n=-1$.

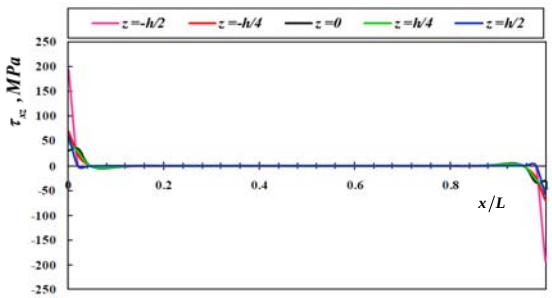

Fig. 13
Shear stress distribution in different layers for $n=+1$.

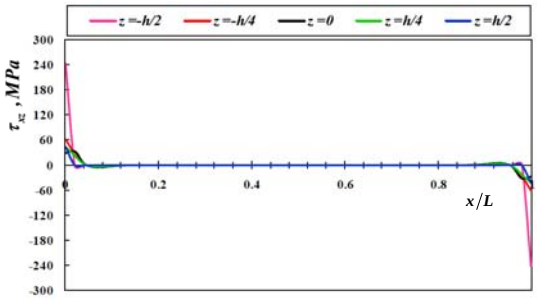

Fig. 14
Shear stress distribution in different layers for $n=-1$.

4.2 Comparison of HSDT and FSDT

Tables1, 2 and 3 present the results of the different solutions at the middle of the heterogeneous cylinder ($x=L/2$) under internal pressure. It is observed that FSDT method has acceptable results for displacements, but the radial and von Mises stresses resulted from FSDT show a significant difference by the results calculated from HSDT and FEM solution. This difference increase at layers close to the boundaries and the greatest difference occurs in the internal surface$\left(z=-h/2\right)$. The FSDT solution procedure has been explained in the references [12, 15].

Table 1
Numerical results of radial displacement for $x=L/2$ at different layers based on SDT and FEM.

u_r ,mm	$n=-1$			$n=0$			$n=+1$		
	HSDT	FSDT	FEM	HSDT	FSDT	FEM	HSDT	FSDT	FEM
$z=-h/2$	0.05280	0.05110	0.05288	0.04420	0.04250	0.04425	0.03660	0.03490	0.03659
$z=-h/4$	0.04910	0.04860	0.04912	0.04090	0.04040	0.04093	0.03370	0.03310	0.03368
$z=0$	0.04620	0.04600	0.04623	0.03840	0.03830	0.03845	0.03150	0.03140	0.03157
$z=h/4$	0.04400	0.04340	0.04401	0.03660	0.03610	0.03659	0.03000	0.02970	0.03001
$z=h/2$	0.04230	0.04080	0.04230	0.03510	0.03400	0.03516	0.02880	0.02790	0.02884

Table 2
Numerical results of radial stress for $x=L/2$ at different layers based on SDT and FEM.

σ_r ,MPa	$n=-1$			$n=0$			$n=+1$		
	HSDT	FSDT	FEM	HSDT	FSDT	FEM	HSDT	FSDT	FEM
$z=-h/2$	-77.751	7.228	-80.000	-77.211	6.738	-80.000	-76.347	6.114	-80.000
$z=-h/4$	-47.322	-14.019	-46.514	-50.836	-12.349	-49.782	-54.364	-10.700	-52.920
$z=0$	-24.759	-27.337	-24.826	-28.158	-27.619	-28.164	-31.723	-27.516	-31.610
$z=h/4$	-9.633	-35.801	-10.198	-11.321	-40.112	-12.168	-13.014	-44.331	-14.333
$z=h/2$	-1.135	-41.180	0.000	-1.754	-50.523	0.000	-2.824	-61.146	0.000

Table 3
Numerical results of von Mises Stress for $x=L/2$ at different layers based on SDT and FEM.

σ_{VMS} ,MPa	$n=-1$			$n=0$			$n=+1$		
	HSDT	FSDT	FEM	HSDT	FSDT	FEM	HSDT	FSDT	FEM
$z=-h/2$	291.64	246.61	289.50	249.67	204.72	250.90	212.26	167.66	216.12
$z=-h/4$	209.60	193.12	209.27	199.50	180.35	199.01	188.01	166.16	187.31
$z=0$	154.72	155.25	154.84	161.98	161.09	162.04	167.47	164.90	167.48
$z=h/4$	117.48	127.53	117.73	134.46	145.56	134.84	151.79	163.89	152.36
$z=h/2$	92.090	93.477	92.412	115.00	132.83	114.31	141.79	163.14	139.48

5 CONCLUSIONS

In this research, the heterogeneous hollow cylinders with radially power varying elastic modulus, have been solved by HSDT and FEM, and have been compared with homogenous cylinders. In the present study, the advantages as well as the disadvantages of the plane elasticity theory (PET) for hollow thick-walled cylindrical shells have been indicated. Regarding the problems which could not be solved through PET, the solution based on the HSDT is suggested. Also the effect of the order of applied approximation based on shear deformation theory on the results has been investigated. At the boundary areas of a thick- walled cylinder with clamped-clamped ends, having constant thickness and uniform pressure, given that displacements and stresses are dependent on radius and length, use cannot be made of PET, and SDT must be used. The shear stress in boundary areas cannot be ignored, but in areas further away from the boundaries, it can be ignored. Therefore, the displacements and stresses at points near the boundaries are different from the other areas under the effect of shear stresses resulted from boundary conditions and the PET can be used, provided that the shear strain is zero. The maximum displacements and the von Mises stresses of the whole areas of the cylinder occur in the internal surface. The cylinder made of heterogeneous materials with positive values of *n* have better behavior than the negative one because of less value of displacements and stresses resulted from these materials. Furthermore, usage of the materials with lower value of $|n|$ causes decrease in subsequent stresses and displacements in the cylinder and would be more convenient for industrial applications. The analytical solutions and the solutions carried out through the FEM show good agreement.

APPENDIX A

$$[A]=\begin{bmatrix}[A_{11}]_{4*4} & [A_{12}]_{4*4}\\ [A_{21}]_{4*4} & [A_{22}]_{4*4}\end{bmatrix} \tag{A.1}$$

$$[A_{12}]=[A_{21}]=0 \tag{A.2}$$

$$[A_{11}]_{ij}=\begin{cases} R\lambda'\int_{-h/2}^{h/2}(\bar{r})^n(1-\nu)\left(1+\frac{z}{R}\right)z^{(i+j-2)}dz & i\ ,\ j=2,3,4\\ 0 & else\end{cases} \tag{A.3}$$

$$[A_{22}]_{ij}=\begin{cases} R\lambda'\int_{-h/2}^{h/2}k(\bar{r})^n(1-\nu)\left(1+\frac{z}{R}\right)z^{(i+j-2)}dz & i\ ,\ j=1,2,3,4\end{cases} \tag{A.4}$$

$$[B]=\begin{bmatrix}[B_{11}]_{4*4} & [B_{12}]_{4*4}\\ [B_{21}]_{4*4} & [B_{22}]_{4*4}\end{bmatrix} \tag{A.5}$$

$$[B_{22}]=0 \tag{A.6}$$

$$[B_{21}]=-[B_{12}]^T \tag{A.7}$$

$$[B_{11}]_{ij}=\begin{cases} R\lambda'\int_{-h/2}^{h/2}(\bar{r})^n(1-\nu)\left(1+\frac{z}{R}\right)z^{(i+j-2)}dz & i=1,\ j=2,3,4\\ & j=1,\ i=2,3,4\\ 0 & else\end{cases} \tag{A.8}$$

$$[B_{12}]_{ij}=\begin{cases} 0 & i=1\\ \lambda'\int_{-h/2}^{h/2}(\bar{r})^n\left[z\left(j\nu-(i-1)k\right)+\left(R\left((j-1)\nu-(i-1)k\right)\right)\right]z^{(i+j-3)}dz & else\end{cases} \tag{A.9}$$

$$[C]=\begin{bmatrix}[C_{11}]_{4*4} & [C_{12}]_{4*4}\\ [C_{21}]_{4*4} & [C_{22}]_{4*4}\end{bmatrix} \tag{A.10}$$

$$[C_{21}]=-[C_{12}]^T \tag{A.11}$$

$$[C_{11}]_{ij}=\begin{cases} R\lambda'\int_{-h/2}^{h/2}(\bar{r})^n(1-\nu)\left(1+\frac{z}{R}\right)dz & i\,,j=1 \\ -(i-1)(j-1)R\lambda' k\int_{-h/2}^{h/2}(\bar{r})^n\left(1+\frac{z}{R}\right)z^{(i+j-4)}dz & else \end{cases} \tag{A.12}$$

$$[C_{12}]_{ij}=\begin{cases} \lambda'\int_{-h/2}^{h/2}\nu(\bar{r})^n\,dz & i\,,j=1 \\ \lambda'\int_{-h/2}^{h/2}\nu(\bar{r})^n z^{j-2}\left((j-1)R+jz\right)dz & i=1,\ j=2,3,4 \\ 0 & else \end{cases} \tag{A.13}$$

$$[C_{22}]_{ij}=\left\{-\lambda'\int_{-h/2}^{h/2}(\bar{r})^n\left[\left((i-1)(j-1)(R+z)(1-\nu)\right)+\left((i+j-2)\nu\right)z+\left(\frac{1-\nu}{R+z}\right)z^2\right]z^{(i+j-4)}dz\right. \quad i\ ,\ j=1,2,3,4 \tag{A.14}$$

where the parameters λ' and k are as follows:

$$\lambda'=\frac{E_i}{(1+\nu)(1-2\nu)} \tag{A.15}$$

$$k=\left(\frac{1-2\nu}{2}\right) \tag{A.16}$$

REFERENCES

[1] Mirsky I., Hermann G., 1958, Axially motions of thick cylindrical shells, *Journal of Applied Mechanics-Transactions of the ASME* **25**: 97-102.

[2] Reddy J.N., Liu C.F., 1985, A higher-order shear deformation theory of laminated elastic shells, *International Journal of Engineering Science* **23**: 319–330.

[3] Greenspon J.E., 1960, Vibration of a thick-walled cylindrical shell, comparison of the exact theory with approximate theories, *Journal of the Acoustical Society of America* **32**(5): 571-578.

[4] Fukui Y., Yamanaka N., 1992, Elastic analysis for thick-walled tubes of functionally graded materials subjected to internal pressure, *The Japan Society of Mechanical Engineers Series I* **35**(4): 891-900.

[5] Simkins T.E., 1994, Amplifications of flexural waves in gun tubes, *Journal of Sound and Vibration* **172**(2): 145-154.

[6] Eipakchi H.R., Rahimi G.H., Khadem S.E., 2003, Closed form solution for displacements of thick cylinders with varying thickness subjected to nonuniform internal pressure, *Structural Engineering and Mechanics* **16**(6): 731-748.

[7] Eipakchi H.R., Khadem S.E., Rahimi G.H., 2008, Axisymmetric stress analysis of a thick conical shell with varying thickness under nonuniform internal pressure, *Engineering Mechanics* **134**: 601-610.

[8] Hongjun X., Zhifei S., Taotao Z., 2006 , Elastic analyses of heterogeneous hollow cylinders, *Journal of Mechanics, Research Communications* **33**(5): 681-691.

[9] Zhifei S., Taotao Z., Hongjun X., 2007, Exact solutions of heterogeneous elastic hollow cylinders, *Composite Structures* **79**(1): 140-147.

[10] Tutuncu N., 2007, Stresses in thick-walled FGM cylinders with exponentially-varying properties, *Engineering Structures* **29**: 2032-2035.

[11] Ghannad M., Rahimi G.H., Khadem S.E., 2010, General plane elasticity solution of axisymmetric functionally graded cylindrical shells, *Journal of Modares Technology and Engineering* **10**(3): 31-43 (in Persian).

[12] Ghannad M., Rahimi G.H., Khadem S.E., 2010, General shear deformation solution of axisymmetric functionally graded cylindrical shells, *Journal of Modares Technology and Engineering* **10**(4): 13-26 (in Persian).

[13] Zamaninejad M., Rahimi G.H., Ghannad M., 2009, Set of field equations for thick shell of revolution made of functionally graded materials in curvilinear coordinate system, *Mechanika* **3**(77): 18-26.

[14] Ghannad M., Zamani Nejad M., Rahimi G.H., 2009, Elastic solution of axisymmetric thick truncated conical shells based on first-order shear deformation theory, *Mechanika* **5**(79): 13-20.

[15] Ghannad M., Zamani Nejad M., 2010, Elastic analysis of pressurized thick hollow cylindrical shells with clamped-clamped ends, *Mechanika* **5**(85): 11-18.

[16] Eipakchi H.R., 2010, Third-order shear deformation theory for stress analysis of a thick conical shell under pressure, *Journal of Mechanics of materials and structures* **5**(1): 1-17.

[17] Ghannad M., Rahimi G.H., Zamani Nejad M., 2012, Determination of displacements and stresses in pressurized thick cylindrical shells with variable thickness using perturbation technique, *Mechanika* **1**(18): 14-21.